Intermolecular Alkene and Alkyne Hydroacylation with β-S-Substituted Aldehydes: Mechanistic Insight into the Role of a Hemilabile P–O–P Ligand

Gemma L. Moxham,[a] **Helen Randell-Sly,**[a] **Simon K. Brayshaw,**[a]
Andrew S. Weller,*[a, c] **and Michael C. Willis***[a, b]

Abstract: A straightforward to assemble catalytic system for the intermolecular hydroacylation reaction of β-S-substituted aldehydes with activated and unactivated alkenes and alkynes is reported. These catalysts promote the hydroacylation reaction between β-S-substituted aldehydes and challenging substrates, such as internal alkynes and 1-octene. The catalysts are based upon [Rh(cod)(DPEphos)][ClO$_4$] (DPEphos = bis(2-diphenylphosphinophenyl)-ether, cod = cyclooctadiene) and were designed to make use of the hemilabile capabilities of the DPEphos ligand to stabilise key acyl–hydrido intermediates against reductive decarbonylation, which results in catalyst death. Studies on the stoichiometric addition of aldehyde (either *ortho*-HCOCH$_2$CH$_2$SMe or *ortho*-HCOC$_6$H$_4$SMe) and methylacrylate to precursor acetone complexes [Rh(acetone)$_2$(DPEphos)][X] [X = *closo*-CB$_{11}$H$_6$Cl$_6$ or [BAr$^F_4$] (Ar^F = 3,5-(CF$_3$)$_2$C$_6$H$_3$)] reveal the role of the hemilabile DPEphos ligand. The crystal structure of [Rh(acetone)$_2$-(DPEphos)][X] shows a *cis*-coordinated diphosphine ligand with the oxygen atom of the DPEphos distal from the rhodium. Addition of aldehyde forms the acyl hydride complexes [Rh-(DPEphos)(COCH$_2$CH$_2$SMe)H][X] or [Rh(DPEphos)(COC$_6$H$_4$SMe)H][X], which have a *trans*-spanning DPEphos ligand and a coordinated ether group. Compared to analogous complexes prepared with dppe (dppe = 1,2-bis(diphenylphosphino)ethane), these DPEphos complexes show significantly increased resistance towards reductive decarbonylation. The crystal structure of the reductive decarbonylation product [Rh(CO)(DPEphos)(EtSMe)][*closo*-CB$_{11}$H$_6$I$_6$] is reported. Addition of alkene (methylacrylate) to the acyl–hydrido complexes forms the final complexes [Rh(DPEphos)(η^1-MeSC$_2$H$_4$-η^1-COC$_2$H$_4$CO$_2$Me)][X] and [Rh-(DPEphos)(η^1-MeSC$_6$H$_4$-η^1-COC$_2$H$_4$-CO$_2$Me)][X], which have been identified spectroscopically and by ESIMS/MS. Intermediate species in this transformation have been observed and tentatively characterised as the alkyl–acyl complexes [Rh(CH$_2$CH$_2$CO$_2$Me)-(COC$_2$H$_4$SMe)(DPEphos)][X] and [Rh(CH$_2$CH$_2$CO$_2$Me)(COC$_6$H$_4$SMe)-(DPEphos)][X]. In these complexes, the DPEphos ligand is now *cis* chelating. A model for the (unobserved) transient alkene complex that would result from addition of alkene to the acyl–hydrido complexes comes from formation of the MeCN adducts [Rh-(DPEphos)(MeSC$_2$H$_4$CO)H(MeCN)][X] and [Rh(DPEphos)(MeSC$_6$-H$_4$CO)H(MeCN)][X]. Changing the ligand from DPEphos to one with a CH$_2$ linkage, [Ph$_2$P(C$_6$H$_4$)]$_2$CH$_2$, gave only decomposition on addition of aldehyde to the acetone precursor, which demonstrated the importance of the hemiabile ether group in DPEphos. With [Ph$_2$P(C$_6$H$_4$)]$_2$S, the sulfur atom has the opposite effect and binds too strongly to the metal centre to allow access to productive acetone intermediates.

Keywords: decarbonylation · heterogeneous catalysis · hydroacylation · phosphane complexes · rhodium

[a] Dr. G. L. Moxham, Dr. H. Randell-Sly, Dr. S. K. Brayshaw,
Dr. A. S. Weller, Dr. M. C. Willis
Department of Chemistry, University of Bath
Bath, BA2 7AY (UK)
Fax: (+44)1865272690
E-mail: andrew.weller@chem.ox.ac.uk
michael.willis@chem.ox.ac.uk

[b] Dr. M. C. Willis
Department of Chemistry, University of Oxford
Chemistry Research Laboratories
Oxford, OX1 3TA (UK)

[c] Dr. A. S. Weller
Department of Chemistry, University of Oxford
Inorganic Chemistry Laboratories, Oxford, OX1 3QR (UK)

Supporting information for this article is available on the WWW under http://dx.doi.org/10.1002/chem.200800738. It contains full experimental and characterisation data for all the new complexes and the solid-state structure of **1**[CbBr$_6$].

Introduction

The transition-metal-catalysed hydroacylation of alkenes and alkynes with aldehydes is an example of a process that combines efficient C−H activation coupled with C−C bond formation, and yields a product with an attractive ketone functionality [Eq. (1)].[1] Although it has attracted significant attention over the last twenty years, the reaction has not enjoyed widespread synthetic use due to the limited set of substrates that can be used. This restriction is largely due to the competing reaction to hydroacylation: metal-mediated reductive decarbonylation. This is problematic in that it is an irreversible process (an alkane is lost) forming metal–carbonyl complexes that are generally inactive or at the very best poor hydroacylation catalysts. A major aspect of the development of hydroacylation as a viable synthetic protocol has been efforts directed to suppress reductive decarbonylation.
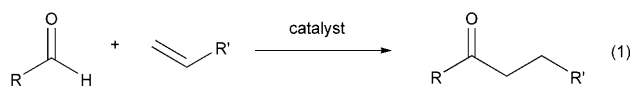
Detailed mechanistic studies of the hydroacylation reaction remain scarce. An early report by Bosnich on intramolecular hydroacylation by using the "[Rh(dppe)]$^+$"[2] catalyst (dppe = 1,2-bis(diphenylphosphino)ethane) and 4-pentenal used deuterium-labelling studies to suggest a likely mechanism (Scheme 1), although no intermediates were definitively characterised spectroscopically. Reductive elimination of the ketone product was suggested to be the turnover limiting step (**D**→**A**, Scheme 1). Very recent calculations by

Morehead and Sargent support this mechanism and also provide insight into the reasons why decarbonylation from intermediates, such as **C** is the less-dominant route under certain conditions of solvent and substrate concentration.[3] Brookhart has studied intermolecular hydroacylation by using [M(η^5-C$_5$Me$_4$X)(η^2-H$_2$C=CHSiMe$_3$)$_2$] complexes (X = Me, CF$_3$; M = Co[4] Rh[5]) with the reductive elimination of the ketone again the turnover-limiting step (**J**→**F**). He also showed that judicious functionalisation of the cyclopentadienyl ligand with electron-withdrawing groups can promote the rate of reductive elimination.[5] The organometallic products of the reductive decarbonylation have been identified, respectively, as cationic [Rh(CO)$_2$(dppe)]$^+$ and the dimer [M(η^5-C$_5$Me$_5$)(CO)]$_2$ (M = Co, Rh) in each system. Both are inactive in the hydroacylation cycle.

The non-productive catalyst decomposition pathway of reductive deacarbonylation requires two processes to occur: deinsertion of the carbonyl group in the acyl hydride to form an alkyl or aryl hydrido carbonyl, followed by reductive elimination of an alkane. Both processes require coordinatively unsaturated metal centres. Deinsertion of a carbonyl requires a vacant site *cis* to the acyl (Scheme 2a),[6,7] whereas reductive elimination of alkanes in neutral or cationic six coordinate d^6 complexes also requires ligand dissociation prior to the rate-determining bond-formation step (Scheme 2b).[8,9] Brookhart has shown that carbonyl deinsertion is reversible in certain hydroacylation systems, and indeed the metal–carbonyl is a resting state for the catalytic cycle (**I**, Scheme 1),[4,5] whereas reversible decarbonylation has been used to account for deuterium scrambling in intermolecular hydroacylation using the "[Rh(dppe)]$^+$" catalyst.[2a,3,10] Thus, it is the irreversible reductive elimination of the alkane that results in ultimate catalyst death. Given that
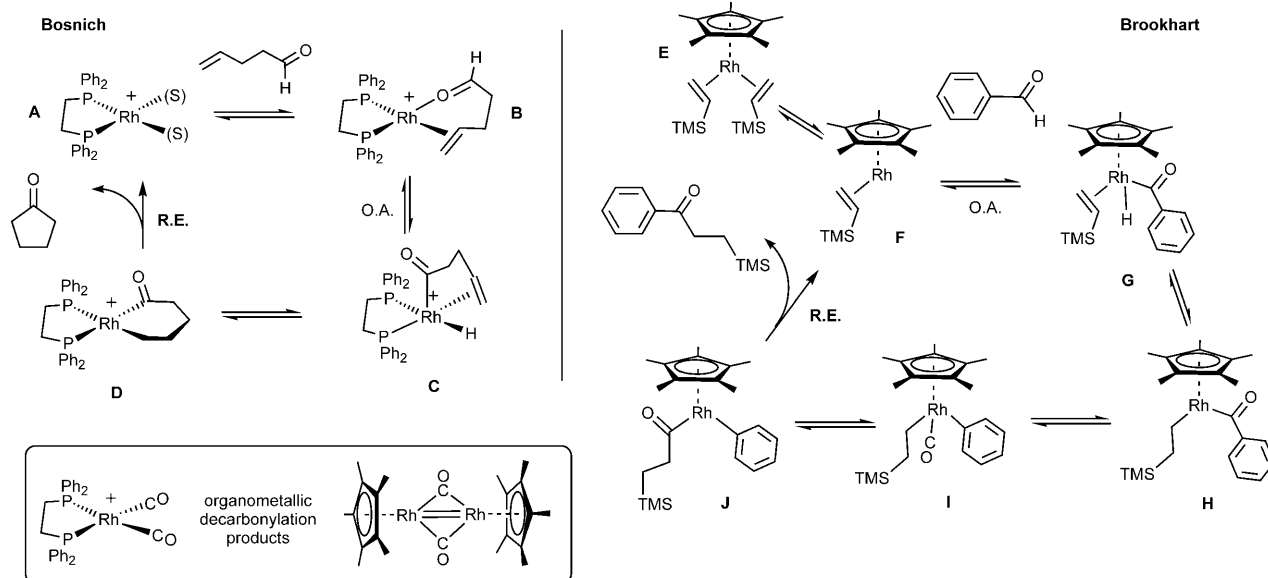
Scheme 1. Abbreviated catalytic cycles for the Rh^I-catalysed hydroacylation of alkenes. The catalytically inactive organometallic products of decarbonylation that is competitive with the hydroacylation cycle are also shown. O.A. = oxidative addition, R.E. = reductive elimination. The turnover-limiting step in both cycles has been determined to be the reductive elimination of the ketone product. Anions have been omitted from the left-hand cycle.

a)

b)
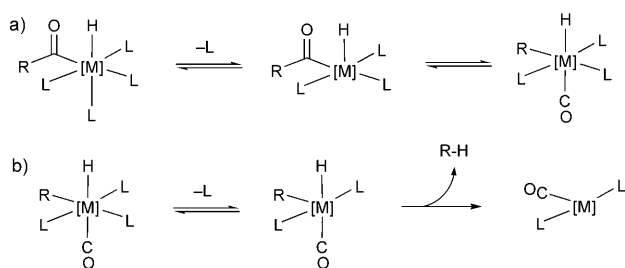
Scheme 2. Carbonyl deinsertion (a) and alkane reductive elimination (b).

rate-determining reductive elimination of the product, substrate binding and reductive decarbonylation all require coordinative unsaturation,[9] the challenge is to establish how productive hydroacylation can be engineered to be favourable over reductive decarbonylation.

Chelation control[11] in intramolecular hydroacylation reactions with 4-pentenals is one answer. This approach was initially reported by Milstein,[12] Bosnich[2a, 13] and James[14] and then developed into asymmetric variants.[15] Intramolecular hydroacylation has also been reported on other, related, systems.[16] Scheme 1 shows the catalytic scheme for the Bosnich system, in which chelation suppresses reductive decarbonylation to such an extent that reasonable catalytic turnover may be achieved. However the fact that this reaction appears specific for the formation of cyclopentanones and is not intermolecular limits its utility. Chelation control has also been used for intermolecular hydroacylation, which has greater synthetic utility. First noted by Suggs[1a] and developed by others,[17–20] the control arises from constraining the acyl within a five-membered metallacycle, which suppresses decarbonylation due to the necessity of this process forming a strained, four-membered, ring. Decarbonylation is also attenuated by coordinating solvent or substrate that can temporarily block the vacant site needed for decarbonylation. Miller noted that the addition of excess ethene to the [RhCl(PPh$_3$)$_3$]-catalysed intramolecular hydroacylation of 4-pentenal increased the yield of desired product,[21a,b] and similar effects have been noted for intermolecular variations,[21c] whereas Bosnich found that excess substrate can retard the reaction while also extending the lifetime of the "[Rh(dppe)]$^+$" catalyst,[2a, 13] suggesting that both substrate inhibition and resistance to decarbonylation occur by blocking a vacant site. Recent computational work presents a slightly differing view and suggests that substrate binding to intermediates such as **D** (Scheme 1) actually facilitates reductive elimination of the product by preferentially lowering the barrier to this process relative to that of decarbonylation.[3] The presence of excess substrate has also been shown to halt reductive decarbonylation in systems based upon [Co(η^5-C$_5$Me$_5$)(η^2-H$_2$C=CHSiMe$_3$)$_2$].[4]

Recent work by one of our groups[18, 20] has made use of the Bosnich [Rh(acetone)$_2$(dppe)]$^+$ catalyst system combined with chelate control with β-S-substituted aldehydes to deliver intermolecular hydroacylation reactions. Although this method has advantages over previous protocols, in that

alkyl aldehydes can be used under mild conditions, several limitations still remain, the most significant of which is that alkynes or electron-poor alkenes are needed to achieve good reactivity. We postulated that by removing decomposition pathways open to the catalyst, such as reductive decarbonylation, longer-lived catalysts would result that would be able to couple more challenging substrates. Given that many of the catalytic intermediates in Scheme 1 have open coordination sites and are electronically unsaturated, we also postulated that stability towards reductive decarbonylation might be deliberately engineered into the catalyst by providing latent stabilisation from a hemilabile ligand (Scheme 3). This would result in a similar scenario to that observed with excess substrate but would provide more control without relying on substrate concentration.
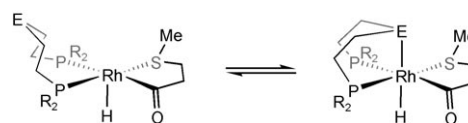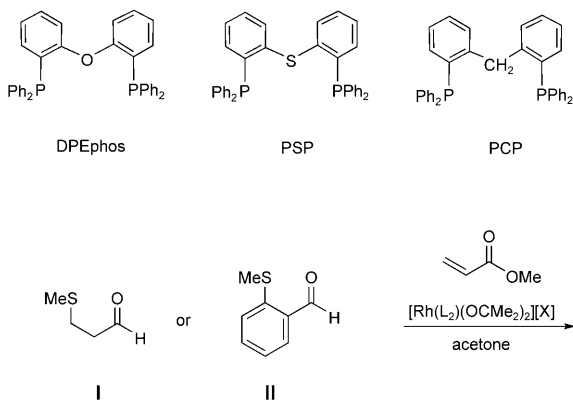

Scheme 3. Suggested hemilabile-ligand protection for the hydroacylation catalyst system.

Hemilabile ligands[22] can potentially provide latent coordinate and electronic protection during catalysis.[23, 24] Our approach, within the context of the hydroacylation reaction, is to use a ligand that would weakly stabilise key coordinatively unsaturated intermediates but move away to allow approach of substrates to the metal centre during the appropriate part(s) of the cycle. The ligand should also be conformationally flexible enough to allow the metal centre to cycle through a number of geometries/oxidation states during catalysis (e.g. Scheme 1). A survey of possible ligands identified DPEphos (DPEphos = bis(2-diphenylphosphinophenyl)ether) as a promising initial candidate as it has been established to behave in a hemilabile manner and can support a range of metal geometries.[25,26] In addition to DPEphos stabilising key unsaturated intermediates, this relatively large biteangle ligand might also have an effect in promoting the turnover limiting reductive elimination step.[25]

This paper details our mechanistic studies into the use of DPEphos, and related, cationic complexes of Rh^I in the hydroacylation reactions with β-S-substituted aldehydes. Intermediates on the catalytic hydroacylation cycle have been identified by NMR spectroscopy, ESIMS and X-ray crystallography. The decarbonylation pathways available to some of these intermediates have also been studied, and the influence that the hemilabile ligand, the aldehyde and the counterion have on complex stability and catalytic turnover are all explored. We also report the development of a practicable catalyst for selected, challenging, intermolecular hydroacylation reactions. We have not performed a detailed kinetic study on these systems and the results presented are a qualitative overview of the catalytic cycle. Aspects of this work have been communicated.[19]

Results and Discussion

To explore the role of the hemilabile ligand, we chose to study the intermolecular hydroacylation reaction between the activated alkene methyl acrylate and the β-substituted aldehydes 3-(methylthio)propionaldehyde **I** or 2-(methylthio)benzaldehyde **II** to afford the ketones **III** and **IV**, respectively [Eq. (2)]. The entry point into our catalytic systems are salts of the general formula [Rh(L$_2$)(nbd)][X] (nbd=norbornadiene) in which L$_2$ is a suitable, hemilabile ligand and [X]$^-$ is a non-coordinating anion, such as [*closo*-CB$_{11}$H$_6$X$_6$]$^-$ (X=halogen),[27,28] [BAr$^F_4$]$^-$ (Ar^F=3,5-(CF$_3$)$_2$C$_6$H$_3$), [PF$_6$]$^-$ or [ClO$_4$]$^-$. For the purposes of this study, we have principally used the [*closo*-CB$_{11}$H$_6$X$_6$]$^-$ (X= Cl, Br, I) and [BAr$^F_4$]$^-$ anions as these often readily offer crystalline materials and can be used interchangeably for the stoichiometric mechanistic studies. From a practical viewpoint, the [ClO$_4$]$^-$ anion serves well in catalytic applications (see sections Evaluation of precatalysts in a benchmark hydroacylation reaction and Applications to organic synthesis—representative examples), although we show there is a notable counterion effect on the overall rate of catalysis. The carborane anions all show ^{11}B{^{1}H} NMR spectra that indicate that they are not bound to the metal centres.[28] The phosphine ligands used for this study are DPEphos, PSP and PCP, and were chosen for the variation of donor properties (O, S or CH$_2$) of the hemilabile ligands. Replacing −O− with −CH$_2$− or −S− groups forms ligands with similar bite angles but very different hemilabile properties.

Evaluation of precatalysts in a benchmark hydroacylation reaction: We selected the combination of β-MeS-substituted propanal (**I**) and methyl acrylate as the benchmark hydroacylation process and used this reaction to evaluate precatalysts [Rh(DPEphos)(nbd)][ClO$_4$], [Rh(PSP)(nbd)][ClO$_4$] and [Rh(PCP)(nbd)][ClO$_4$], along with the Bosnich catalyst [Rh(dppe)(nbd)][ClO$_4$] (Table 1). Active catalysts were gen-
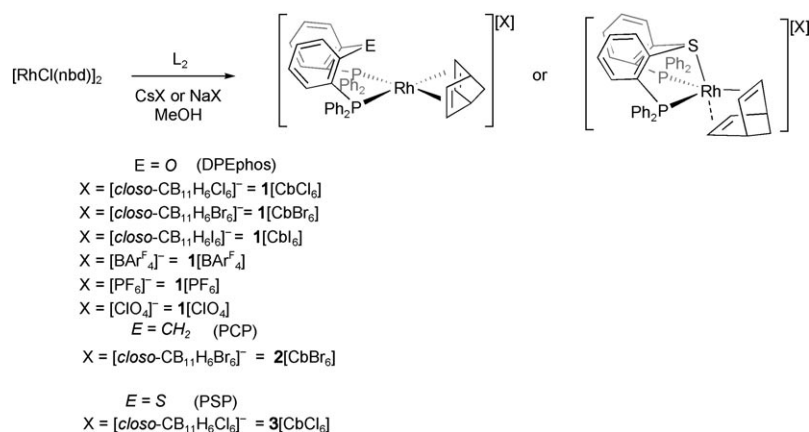
Table 1. Benchmark catalyst evaluation.[a]

Entry	Precatalyst	Conversion [%][b]	t
1	[Rh(dppe)(nbd)][ClO$_4$]	100[c]	90 min
2	[Rh(DPEphos)(nbd)][ClO$_4$]	100	60 min
3	[Rh(nbd)(PSP)][ClO$_4$]	0	48 h
4	[Rh(nbd)(PCP)][ClO$_4$]	0	48 h
5[d]	[RhCl(cod)]$_2$/DPEphos/Ag[ClO$_4$]	100	90 min

[a] Conditions: aldehyde (1.0 equiv), methyl acrylate (2.0 equiv), catalyst (5 mol%), acetone, 55 °C. Catalysts were generated from the corresponding precatalysts by hydrogenation (1 atm, 5 min, acetone). See section entitled synthesis of precatalysts for details of their synthesis. [b] Determined by ^{1}H NMR spectroscopy. [c] The product was obtained as a 4:1 mixture of linear/branched isomers. In all other reactions, the product was formed exclusively as the linear compound. [d] Catalyst generated from the simple combination of the three components.

(2)

We first briefly report the initial screening of hemilabile ligand sets in a benchmark hydroacylation reaction that demonstrates the potential of the DPEphos ligand. We then move on to discuss in detail the synthesis, characterisation and reactivity of species directly relevant to the catalytic cycle by stoichiometric addition of aldehyde and alkene to suitable DPEphos-containing precatalyts. Finally, the utility of these DPEphos catalysts in challenging hydroacylation reactions is demonstrated.

erated by adding H$_2$, elimination of norborane and formation of the corresponding acetone adducts, [Rh(L$_2$)-(acetone)$_2$][ClO$_4$]. The reaction with the Bosnich catalyst took 90 minutes to achieve 100% conversion (entry 1). Employing the DPEphos-derived precatalyst achieved the same conversion after 60 minutes (entry 2). Monitoring the reactions by ^{1}H NMR spectroscopy confirmed this difference in rate. Reactions employing the thio- (PSP) and methylene-bridged (PCP) ligands failed to deliver any of the expected product (entries 3 and 4). The final entry (entry 5) demonstrated that the simple combination of [RhCl(cod)]$_2$, DPEphos and Ag[ClO$_4$] generated a catalyst that achieved complete conversion in 90 minutes (entry 5). ^{31}P{^{1}H} NMR spectroscopy of this in situ generated catalyst showed the formation of [Rh(cod)(DPEphos)]-[ClO$_4$], which on addition of aldehyde formed the active species (**6a**[ClO$_4$], vide infra). From a practical perspective, the ability to avoid hydrogenation of a precatalyst significantly adds to the utility of the system (see the section Applications to organic synthesis—representative examples). After having established that the DPEphos-derived system offered an advantage in the benchmark hydroacylation reaction, we moved on to a series of stoichiometric qualitative mechanistic studies in order to understand the basis for this reactivity and especially the role of the hemilabile ligand—if any.

Synthesis of precatalysts: For the stepwise mechanistic study, well-defined and pure precursor complexes were required. So although from a practical viewpoint (see the section Applications to organic synthesis—representative examples) catalysts are best prepared in situ from [RhCl-(cod)]$_2$/L$_2$ and Ag[X] in acetone, for this study the cleanest materials come from first preparing the complexes [Rh(L$_2$)-(nbd)][X] **1**[X]–**3**[X] (Scheme 4). The related complex [Rh-(cod)(DPEphos)][BF$_4$] has been reported previously.[29] The ^{31}P{^{1}H} NMR spectroscopic data for salts **1**[X] show no variation with anion. Along with **2**[CbBr$_6$] they show doublets at $\delta = 17.0$ (d, J(RhP)$ = 159$ Hz, **1**[X]) and 23.0 ppm (d, J(RhP)$ = 166$ ppm, **2**[X]), with coupling to ^{103}Rh consistent with coordination of phosphine to a Rh^I square-planar centre. The molecular crystal structure of **1**[CbBr$_6$] (Table 2) displays the expected square-planar motif, with no close Rh···O contacts (Rh−O 3.523 Å) (see the Supporting Information). Interestingly, the ^{1}H NMR spectrum of **2**[CbBr$_6$] shows the inequivalent methylene protons of the PCP ligand at two very different chemical shifts, $\delta = 6.24$ and 4.33 ppm, the former shifted downfield compared with the free ligand ($\delta = 4.45$ ppm). Similar chemical-shift differences were noted in the related complex [PdCl$_2$-(PCP)], and while the solid-state structure shows a relatively close C−H(*endo*)···Pd dis-

E = O (DPEphos)
X = [*closo*-CB$_{11}$H$_6$Cl$_6$]$^-$ = **1**[CbCl$_6$]
X = [*closo*-CB$_{11}$H$_6$Br$_6$]$^-$ = **1**[CbBr$_6$]
X = [*closo*-CB$_{11}$H$_6$I$_6$]$^-$ = **1**[CbI$_6$]
X = [BAr$^F_4$]$^-$ = **1**[BAr$^F_4$]
X = [PF$_6$]$^-$ = **1**[PF$_6$]
X = [ClO$_4$]$^-$ = **1**[ClO$_4$]
E = CH$_2$ (PCP)
X = [*closo*-CB$_{11}$H$_6$Br$_6$]$^-$ = **2**[CbBr$_6$]

E = S (PSP)
X = [*closo*-CB$_{11}$H$_6$Cl$_6$]$^-$ = **3**[CbCl$_6$]

Scheme 4. Salts **1**[X]–**3**[X].

Table 2. Crystal structure and refinement data.

	1[CbBr$_6$]	**3**[CbCl$_6$]	**4**[CbCl$_6$]	**6b**[CbBr$_6$]	**7**[CbBr$_6$]	**8a**[CbCl$_6$]
formula	C$_{45}$H$_{44}$B$_{11}$Br$_6$Cl$_2$OP$_2$Rh	C$_{44}$H$_{41.92}$B$_{11}$Cl$_{6.08}$P$_2$RhS	C$_{46}$H$_{51.87}$B$_{11}$Cl$_{6.13}$O$_4$P$_2$Rh	C$_{63}$H$_{57}$B$_{11}$Br$_6$F$_3$O$_2$P$_2$RhS	C$_{41}$H$_{42}$B$_{11}$Br$_6$O$_2$P$_2$RhS	C$_{46}$H$_{50.92}$B$_{11}$Cl$_{6.08}$NO$_3$P$_2$RhS
M_w	1434.92	1102.06	1169.88	1698.37	1362.03	1197.09
specimen [mm]	0.48 × 0.30 × 0.10	0.45 × 0.35 × 0.20	0.30 × 0.20 × 0.20	0.35 × 0.20 × 0.10	0.45 × 0.30 × 0.08	0.28 × 0.23 × 0.20
crystal system	monoclinic	orthorhombic	triclinic	monoclinic	monoclinic	monoclinic
space group	$P2_1/c$	$Pbca$	$P\bar{1}$	$P2_1/c$	$C2/c$	$C2/c$
a [Å]	13.2823(2)	20.3691(1)	13.6680(1)	14.1224(2)	25.1370(4)	35.0748(3)
b [Å]	31.7248(4)	18.8427(1)	13.7350(1)	32.9909(3)	13.2248(2)	11.3221(1)
c [Å]	14.2156(2)	25.3130(1)	17.8597(1)	14.4927(2)	30.6433(5)	32.2252(3)
α [°]	90	90	92.8916(3)	90	90	90
β [°]	117.2678(7)	90	106.7497(3)	95.8867(5)	90.2907(7)	110.2554(7)
γ [°]	90	90	116.7593(3)	90	90	90
V [Å^3]	5324.49(13)	9715.35(8)	2802.33(3)	6716.70(15)	10186.7(3)	12005.9(2)
Z	4	8	2	4	8	8
μ [mm^{-1}]	5.020	0.829	0.688	3.954	5.181	0.683
ρ_{calcd} [g cm^{-3}]	1.790	1.507	1.387	1.680	1.776	1.326
$2\theta_{max}$ [°]	57.3	66.2	57.0	54.9	55.2	52.6
N_{total} collected	54 777	201 967	54 423	65 148	39 213	54 980
$N_{independent}$ (R_{int})	12 480 (0.0632)	18 428 (0.0585)	14 013 (0.0451)	15 013 (0.0648)	10 330 (0.0708)	11 996 (0.0680)
N ($I > 2\sigma(I)$)	9867	14 132	11 933	10 469	8287	9621
R_1 ($I > 2\sigma(I)$)	0.0554	0.0301	0.0321	0.0471	0.0585	0.0566
R_1 (all data)	0.0761	0.0496	0.0428	0.0832	0.0772	0.0768
wR_2 ($I > 2\sigma(I)$)	0.1327	0.0727	0.0757	0.1055	0.1415	0.1302
wR_2 (all data)	0.1431	0.0831	0.0804	0.1184	0.1515	0.1394

tance, a ring-current-induced chemical shift was suggested as the reason for the downfield shift.[30] An alternative explanation comes from recent work from the Bercaw group who have classified such interactions as *pre-agostic* with support from structural and computational studies.[31] It is likely that such an interaction is also present in **2**[CbBr$_6$].

By contrast with the other nbd adducts, **3**[CbCl$_6$] shows a downfield-shifted resonance in the ^{31}P{^{1}H} NMR spectrum with reduced coupling to ^{103}Rh, $\delta = 57.5$ ppm (d, J(RhP) = 125 Hz). Both these observations suggest coordination of the sulfur atom to form a five-coordinate 18-electron complex with a tridentate PSP ligand.[32] The solid-state structure confirms this (Figure 1) and shows a pseudo-trigonal bipyramidal coordinated Rh^I centre, with a close rhodium–sulfur
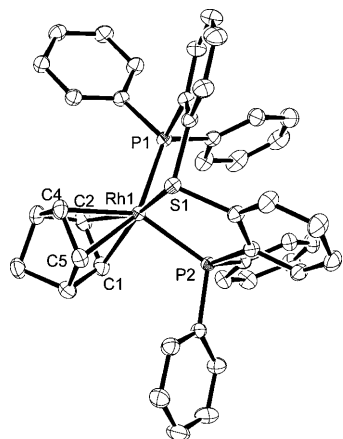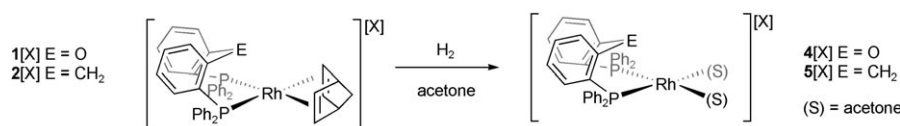

Scheme 5. Generation of acetone adducts. Identity of [X] follows that shown in Scheme 4.
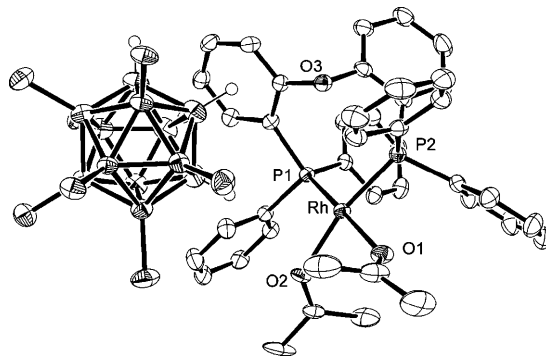

Figure 2. Molecular structure of **4**[CbCl$_6$]. Selected bond lengths [Å]: Rh−O1 2.154(2), Rh−O2 2.126(4), Rh−O3 3.562(2), Rh−P1 2.2019(5), Rh−P2 2.1978(6); selected bond angles [°]: O2-Rh-O1 83.30(12), P2-Rh-P1 96.23(2), O2-Rh-P1 94.42(11), O1-Rh-P2 85.52(5), O1-Rh-P1 174.31(5), O2-Rh-P2 167.70(12). Sum of angles around Rh, 359.47°. The acetone ligands are disordered and only the major component is shown.

Figure 1. Molecular structure of the cationic portion of **3**[CbCl$_6$]. Ellipsoids are drawn at the 50% probability level. The hydrogen atoms and anion have been omitted for clarity. Selected bond lengths [Å]: Rh1−C5 2.167(2), Rh1−C4 2.192(2), Rh1−C1 2.218(2), Rh1−C2 2.230(2), Rh1−S1 2.2955(5), Rh1−P1 2.3487(5), Rh1−P2 2.3489(5), C1−C2 1.387(2), C4−C5 1.415(2); selected bond angles [°]: P1-Rh1-P2 103.38(2), S1-Rh1-P1 85.82(2), S1-Rh1-P2 86.73(2), C4-Rh1-S1 95.25(5), C2-Rh1-S1 156.64(5).

distance (Rh1−S1 2.2955(5) Å) and mutually *cis*-phosphines. ^{31}P{^{1}H} NMR spectroscopy shows resonances at $\delta = 41.8$ ppm (d, J(RhP) = 209 Hz) for **4**[CbCl$_6$] and $\delta = 41.5$ ppm (d, J(RhP) = 202 Hz) for **5**[CbBr$_6$]. The *endo* and *exo* protons for the CH$_2$ linker in **5**[CbBr$_6$] are now observed as being almost isochronous at $\approx \delta = 4.0$ ppm in the ^{1}H NMR spectrum, which suggests that the C−H⋯Rh interaction present in **2**[BAr$^F_4$] is now absent, or at least attenuated significantly. Electrospray ionisation mass spectrometry (ESIMS) of these acetone adducts shows the expected peaks due to the parent cation and loss of one and two acetone molecules. By contrast, salt **3**[CbCl$_6$] does not react with hydrogen (even at ≈ 100 bar H$_2$), which suggests that the sulfur atom is very strongly bound, the 18-electron configuration retained and the oxidative addition of H$_2$ disfavoured. This lack of reactivity correlates with the inactivity of this complex in the benchmark hydroacylation reaction (Table 1) as presumably the active acetone adduct is not formed.

distance (Rh1−S1 2.2955(5) Å) and mutually *cis*-phosphines. The alkene C4/C5 unit and the two phosphines lie in the trigonal plane. 18-electron, Rh^I, complexes with π-accepting ligands have been reported previously.[33]

Addition of H$_2$ to acetone solutions of these nbd adducts was anticipated to remove the strained diene and generate the desired precatalysts, analogous to the Bonsich catalyst.[34] For salts **1**[X] and **2**[X] this is the case and the acetone adducts [Rh(L$_2$)(acetone)$_2$][X] **4**[X] and **5**[X], respectively, can be generated in quantitative yield as determined by NMR spectroscopy (Scheme 5). The reaction is immediate by NMR spectroscopy. A solid-state structure has been obtained for **4**[CbCl$_6$] (Figure 2), which shows no coordination of the ether linkage with the metal centre (Rh⋯O3

Synthesis of acyl–hydrido intermediates: With suitable precursor Rh^I complexes in hand, we next investigated the addition of aldehyde, accepted to be the first step in the catalytic cycle for hydroacylation.[2a,3] Addition of either aldehyde **I** or **II** to acetone solutions of **4**[X] resulted in the immediate (less than 5 minutes) formation of new acyl hydrido species, [Rh(COCH$_2$CH$_2$SMe)(DPEphos)H][X] **6a**[X] and [Rh(COC$_6$H$_4$SMe)(DPEphos)H][X] **6b**[X], in quantitative yield as determined by NMR spectroscopy (Scheme 6). Addition of **I** or **II** to **5**[CbCl$_6$], which offers no hemilabile protection from the CH$_2$ group, immediately (less than 5 minutes) gave a number of unidentified species and no acyl–
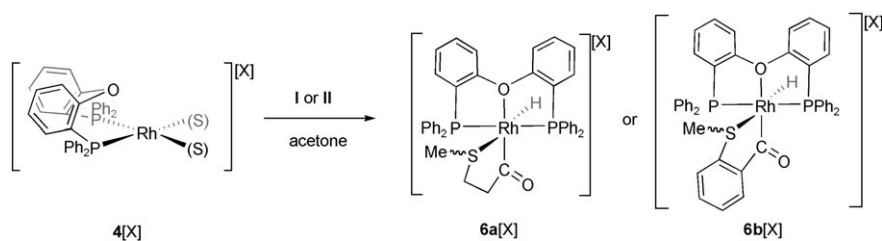
Scheme 6. Formation of new acyl–hydrido species **6a**[X] and **6b**[X]; [X]$^-$ = [*closo*-CB$_{11}$H$_6$Cl$_6$]$^-$.

hydrido complexes. In this case, possible C−H activation of the bridging methylene group may also play a role in the decomposition pathway.[30] This rapid decomposition correlates with the poor performance of this complex in the benchmark reaction (Table 1).

The anions [*closo*-CB$_{11}$H$_6$Br$_6$]$^-$, [*closo*-CB$_{11}$H$_6$Cl$_6$]$^-$, and [BAr$^F_4$]$^-$ were used interchangeably with no effect on the yield or identity of the cationic portion of the products, and the NMR spectroscopic data is discussed for **6a**[CbCl$_6$], although the molecular structure from an X-ray diffraction experiment was obtained for **6b**[CbBr$_6$] (Figure 3). We were unable to obtain a crystal structure for **6a**[X] (with a variety of anions) because of the reductive decarbonylation of the acyl ligand over the timescale of the crystallisation (days, vide infra). The structure of **6b**[CbBr$_6$] shows a meridonial coodination of the DPEphos ligand, with the (located) hydride ligand *trans* to sulfur atom and the acyl ligand *trans* to the ether, which now occupies a coordination site on the metal centre. The rhodium is best described as being in the Rh^{III} oxidation state, whereas the ligand orientations are in accord with *trans*-influence arguments and are also consis-
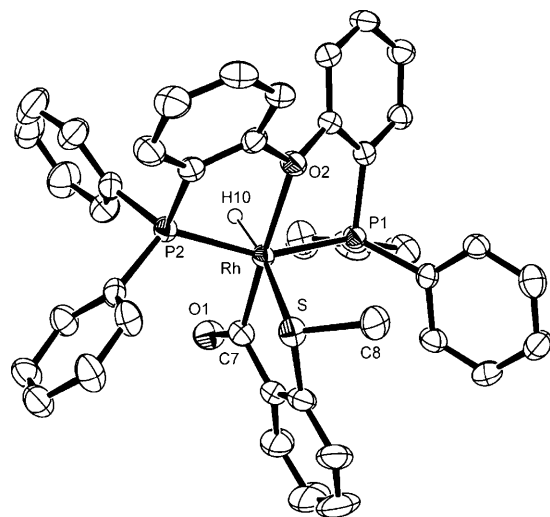

Figure 3. Molecular structure of the cationic portion of **6b**[CbBr$_6$]. Ellipsoids are drawn at the 50 % probability level. The anion and hydrogen atoms other than Rh−H are omitted for clarity. Selected bond lengths [Å]: Rh−H(10) 1.47(4), Rh−O2 2.248(3), Rh−P1 2.293(1), Rh−P2 2.303(1), Rh−S 2.428(1), Rh−C7 1.969(5); selected bond angles [°]: P1-Rh-P2 155.93(5), C7-Rh-S 84.88(14), H(10)-Rh-S 169.7(15), C7-Rh-O2 177.3(2) C8-S-Rh-O2 torsion −48.4(2)

tent with solution NMR spectroscopic data (vide infra). The Rh−O distance (Rh−O2 2.248(3) Å) is ca. 0.1 Å longer than that observed in [Rh-(xantphos)CO][BF$_4$] (2.126(3) Å; xantphos = 9,9-dimethyl-4,5-bis(diphenylphosphino)xanthene),[24] and related compounds.[35] The Rh−C$_{acyl}$ distance, 1.969(5) Å, is similar to other reported Rh^{III}-acyl bond lengths, for example that found in [Rh(P*i*Pr$_3$)$_2$H(COCH$_3$)](OTf).[7] The methyl group on the sulfur atom is canted away from lying in the Rh−S−C$_{acyl}$−O plane, C$_{acyl}$−S−Rh−O$_{ether}$ torsion = 48.4(2)°. This, along with the twist of the DPEphos ligand backbone, makes the phosphine atoms inequivalent in the solid-state. *cis*-Acyl–hydrido complexes formed from addition of an aldehyde to a low-valent rhodium centre are known[1a,9,12,36] and in some cases have been crystallographically characterised.[7,37] However, as far as we are aware, very few have actually been shown to be active in the hydroacylation reaction.[1a,12]

In solution at room temperature, complexes **6a/b**[CbCl$_6$] show similar sets of peaks for the phosphine and hydride ligands in their NMR spectra and only those for **6a**[CbCl$_6$] are discussed in detail. The hydride signal is observed as a doublet of triplets at $\delta = -8.75$ ppm (J(RhH) = 23, J(PH) = ≈ 1 Hz), and one slightly broadened signal is observed for the SMe group at $\delta = 1.56$ ppm. The small coupling to ^{31}P suggests a mutual *cis*-orientation of hydride and phosphine ligands. A ^{1}H-^{1}H COSY spectrum at 298 K revealed a four-bond correlation between the hydride signal and the *S*-methyl group, which suggests that the *trans* orientation of the hydride and thioether observed in the solid-state is retained in solution. The ^{13}C{^{1}H} NMR spectrum displays the acyl carbon atom as a doublet at $\delta = 223.2$ (J(RhC) = 34 Hz), with the expected coupling to the *cis* phosphines presumably small and unresolved. This chemical shift and coupling constant are similar to those reported for related rhodium acyl complexes, such as [Rh(acac)(PPh$_3$)(MeCO)I]$_2$ ($\delta = 212.4$ ppm, J(RhC) = 28 Hz)[38] or [Rh(η^5-C$_5$Me$_5$)(C(O)C$_6$H$_4$CH$_3$)][BAr$^F_4$] ($\delta = 233.2$ ppm, J(RhC) = 29 Hz).[39]

A single resonance is observed in the ^{31}P{^{1}H} NMR spectrum at room temperature that shows coupling to ^{103}Rh. This is at odds with the solid-state structure, which shows inequivalent phosphorus environments. Progressive cooling to 180 K resolves this signal into a tightly-coupled ABX doublet of doublets, showing large ^{31}P–^{31}P coupling (J(RhP) = 125, J(PP) = 305 Hz) for **6a**[CbCl$_6$]. Such a large coupling indicates *trans*-orientated phosphines—as found in the solid-state structure. The hydride signal does not change significantly on cooling, and only one SMe environment is observed. The fluxional process that makes equivalent the phosphorus atoms at room temperature cannot involve breaking of the Rh−P bond (^{103}Rh coupling is observed at

298 K) or the Rh–S bond (a correlation is observed between hydride and SMe). Line-shape analysis affords $\Delta G^+(298\ K)$ for this process, and comparison shows that the order for ease of reorganisation for **6b**[CbCl$_6$] ((32 ± 2.3) kJ mol^{-1}) is less than **6a**[CbCl$_6$] ((42 ± 2.7) kJ mol^{-1}). The thiobenzaldehyde **II** thus results in a lower barrier to reorganisation by ≈ 10 kJ mol^{-1} relative to **I**). ΔS^+ values are close to zero (less the (5 ± 3) J K^{-1} mol^{-1}). Two plausible mechanisms for this reorganisation involve breaking the Rh–O bond to access a conformationally flexible five coordinate intermediate or inversion at the sulfur atom, which if coupled with a twist of the phosphine backbone would render the phosphorus atoms equivalent. Inversion at the sulfur atom is a well-documented process[40,41] and reported barriers are similar to those determined here. The available data does not allow the discrimination of which process is occurring: Rh–O cleavage or inversion at the sulfur atom. Although, as is demonstrated later, the DPEphos ligand can be displaced by excess MeCN, which shows that the Rh–O bond can be broken, we cannot envisage a plausible low-energy pathway that would retain coupling between the hydride and SMe (as is observed at 298 K) and invoke five-coordinate intermediates that interconvert the methyl group from one side to the other. Inversion at the sulfur atom would pass through a planar, sp^2-like at S intermediate. Such an intermediate would be stabilised by the aryl group present in ligand **II**, whereas stabilising (p–d)π conjugation would also be favoured by weakening, although not necessarily breaking, of the Rh–O bond to the hemilabile ligand.[41]

Decarbonylation of the acyl–hydrido complexes: Given that suppressing reductive decarbonylation is central to making a longer-lived catalyst, the stability of the new acyl–hydrido complexes in acetone was studied. Leaving a sample of **6a**-[CbCl$_6$] or **6b**[CbCl$_6$] in acetone for seven days at room temperature caused new compounds to be formed (Scheme 7). These were characterised by NMR spectroscopy and ESIMS to be [Rh(CO)(DPEphos)(EtSMe)][*closo*-CB$_{11}$H$_6$Cl$_6$] (**7a**-[CbCl$_6$]) and [Rh(CO)(DPEphos)(PhSMe)][*closo*-CB$_{11}$H$_6$Cl$_6$] (**7b**[CbCl$_6$]). The molecular structure of **7a**-[CbI$_6$] (the iodo carborane was used to obtain crystals suitable for the diffraction experiment) is shown in Figure 4 and demonstrates a square-planar Rh^I centre with a *cis*-DPE-phos ligand, a carbonyl and methylethylthioether ligand. The last two ligands arise from reductive decarbonylation of the acyl hydride in the starting material. The ^{1}H and ^{31}P{^{1}H} NMR spectra at 220 K are in full accord with the
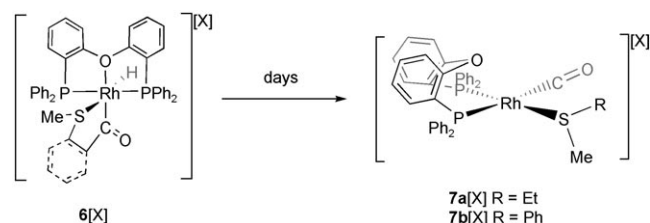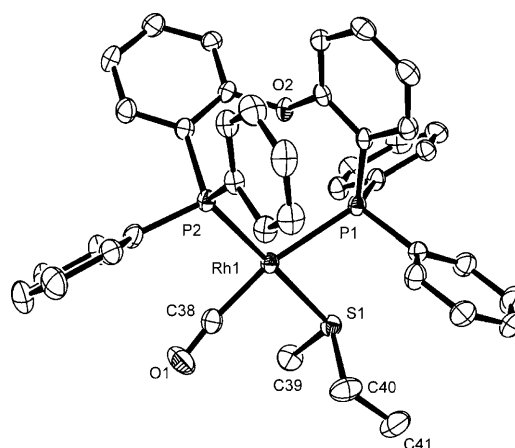

Figure 4. Molecular structure of the cationic portion of **7a**[CbI$_6$] Ellipsoids are drawn at the 50% probability level. The anion and hydrogen atoms have been omitted for clarity. Selected bond lengths [Å]: Rh–C(38) 1.869(4), Rh–S1 2.3694(11), Rh–P1 2.387(1), Rh–P2 2.309(1), Rh–O2 3.525(3); selected bond angles [°]: C(38)-Rh-S1 88.13(14) P2-Rh-P1 98.64(4), C(38)-Rh-P2 90.87(14), S1-Rh-P1 82.27(4).

solid-state structure: two ^{31}P environments are observed at $\delta = 20.7$ and 15.9 ppm that show *cis* ^{31}P–^{31}P coupling (J(PP) = 30 Hz) as well as coupling to ^{103}Rh. The lower-field signal shows a smaller ^{103}Rh–^{31}P coupling constant (150 vs. 125 Hz), which suggests it is due to the phosphorus *trans* to the thioether.[42] Signals due to the thioether group are observed in the ^{1}H NMR spectrum. At room temperature, the ^{31}P{^{1}H} NMR spectrum shows a broad, frequency-averaged, signal that suggests an exchange process with reversible de-coordination of the, now monodentate, thioether being the most likely mechanism. The ESIMS spectrum shows a peak at $m/z = 699.06$ that corresponds to the parent ion minus EtSMe, which further suggests a weakly bound thioether group. Data for **7b**[CbCl$_6$] are broadly similar and suggest a closely related structure.

This reductive decarbonylation was monitored over time by NMR spectroscopy. Solutions of **6a**[CbCl$_6$] and **6b**-[CbCl$_6$], formed in situ by addition of the respective aldehyde **I** or **II** to the acetone adduct **4**[CbCl$_6$], were kept at 298 K and monitored periodically by ^{31}P{^{1}H} and ^{1}H NMR spectroscopy over a period of one week. The disappearance of the hydride peak of the starting materials in the ^{1}H NMR spectrum was monitored and plotted (Figure 5). The ^{31}P{^{1}H} NMR spectrum shows similar time-dependant profiles, with the smooth conversion of **6**[CbCl$_6$] into **7**[CbCl$_6$] observed for both complexes. By way of comparison, the Bonsich system [Rh(acetone)$_2$(dppe)]$^+$ (as the [CbBr$_6$]$^-$ salt) was also studied by adding aldehyde **I** or **II** to acetone solutions of this precatalyst.

Complexes **6a**[CbCl$_6$] and **6b**[CbCl$_6$] reductively decarbonylate to give **7a**[CbCl$_6$] and **7b**[CbCl$_6$], respectively, following first-order kinetics. Complex **6a**[CbCl$_6$] decarbonylates significantly faster than **6b**[CbCl$_6$] ($k = (1.0 \times 10^{-5} \pm 0.1)$ vs. ($1.2 \pm 0.1 \times 10^{-6}$) s^{-1}, respectively), the aryl backbone in **6b**[CbCl$_6$] clearly inhibiting decarbonylation, as is to be ex-

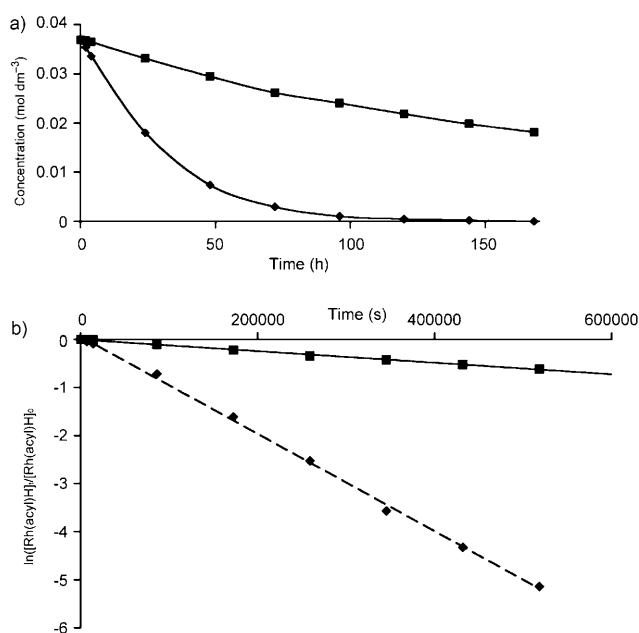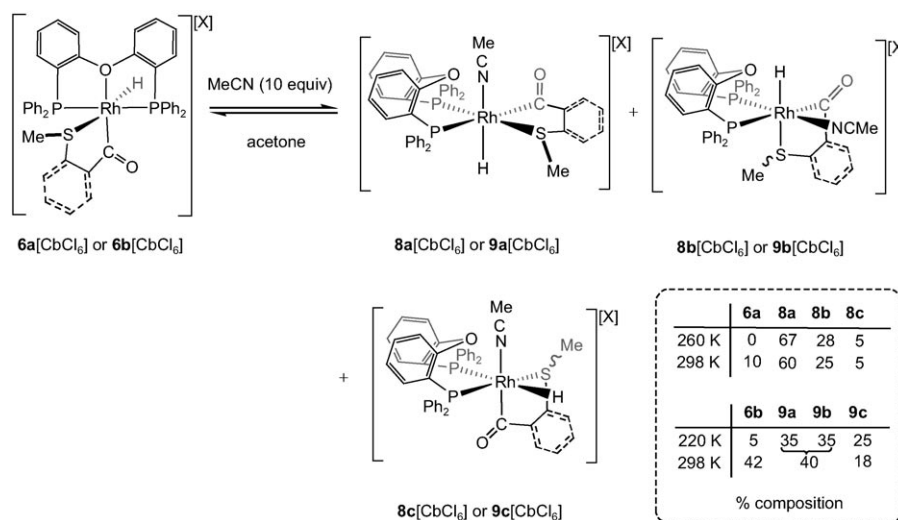Scheme 7. Formation of products **7a**[X] and **7b**[X].

Figure 5. a) Decomposition of the acyl–hydride intermediates over one week. Concentrations calculated from NMR spectroscopic integrals by using an internal standard. b) Plot of $\ln([\text{Rh(acyl)hydride}]_t/[\text{Rh-(acyl)hydride}]_0)$ versus time to obtain rate constant, k, for the decomposition of the acyl–hydride complexes of the DPEphos ligand. ♦: **6a**[CbCl$_6$]; ■: **6b**[CbCl$_6$].

pected for a more rigid system.[1] For the dppe system, a complex mixture is formed on addition of aldehyde to [Rh-(acetone)$_2$(dppe)][CbBr$_6$] for which we were not able to definitively assign signals due to an acyl–hydride species. ESIMS of this mixture indicated that the product of reductive decarbonylation [Rh(CO)(dppe)(SMeEt)]$^+$ had been formed. Noteworthy is that acyl–hydrido intermediates were not observed in the original report of addition of 4-pentenal to [Rh(acetone)$_2$(dppe)][ClO$_4$].[2a]

Displacement of the hemilabile oxygen ligand by using MeCN: As we show in the next section, addition of alkene to **6**[CbCl$_6$] rapidly affords the ultimate products of hydroacylation, which means that the simple alkene adducts are not observed. We have modelled the coordination of alkene to the metal centre by addition of acetonitrile. Adding ten equivalents of MeCN to acetone solutions of **6a**[CbCl$_6$] or **6b**[CbCl$_6$] resulted in displacement of the bound oxygen atom and the formation of the adducts [Rh-(DPEphos)(MeSC$_2$H$_4$CO)H-(MeCN)][closo-CB$_{11}$H$_6$Cl$_6$] (**8**-[CbCl$_6$]) and [Rh-

(DPEphos)(MeSC$_6$H$_4$CO)H(MeCN)][closo-CB$_{11}$H$_6$Cl$_6$] (**9**-[CbCl$_6$]) as an equilibrium mixture of three isomers (**a**, **b** and **c**) and the starting materials (Scheme 8, inset table).[43] Excess MeCN ($\approx$100 equivalents) pushes the equilibrium completely over to the products.

The isomers of **8**[CbCl$_6$] and **9**[CbCl$_6$] have been identified by ^{1}H and ^{31}P NMR spectroscopy as those shown in Scheme 8. At room temperature, the MeCN adducts show as broad peaks in the ^{31}P{^{1}H} NMR spectrum, whereas **6**-[CbCl$_6$] remains sharp, demonstrating that the rate of exchange between the adducts is approaching the NMR timescale but that with **6**[CbCl$_6$] is slow. On cooling, sharp peaks are resolved, and the ratio of the adducts to starting material changes in favour of the MeCN complexes (Scheme 8). Warming restores the original concentrations. A large ^{31}P–^{1}H coupling observed for the hydride signals of isomers **8c**[CbCl$_6$] and **9c**[CbCl$_6$] ($J(\text{PH}) = \approx 160$ Hz), which appear as a well-resolved doublet of doublet of doublets for **9c**-[CbCl$_6$], indicate a hydride trans to one phosphine and cis to the other, whereas those for **8a/b**[CbCl$_6$] and **9a/b**[CbCl$_6$] show only smaller cis coupling to ^{31}P. The ^{31}P{^{1}H} NMR spectrum demonstrates that the phosphine ligands in all the isomers lie cis to one another as indicated by the two different environments observed for each isomer, which also show mutual cis ^{31}P–^{31}P coupling. Each pair of phosphorus environments shows one large and one small $J(\text{RhP})$ coupling (for example, 157/65, 150/66 and 155/65 for **9a**[CbCl$_6$], **9b**[CbCl$_6$] and **9c**[CbCl$_6$], respectively), which suggests structures in which one phosphorus atom is opposite a high trans-influence ligand (acyl or hydride: low $J(\text{RhP})$), whereas the other is trans to the thioether or MeCN (larger J-(RhP)). Only three peaks are observed for the SMe groups between $\delta = 1.8$ and 1.4 ppm in the ^{1}H NMR spectrum, which is accounted for by a coincidence of resonances for two of the species. Owing to the complexity of the system, ^{13}C{^{1}H} NMR spectroscopy was not useful in determining the structures of the products. Integrating over all the iso-

	6a	8a	8b	8c
260 K	0	67	28	5
298 K	10	60	25	5

	6b	9a	9b	9c
220 K	5	35	35	25
298 K	42	40		18

% composition

Scheme 8. At 298 K, the signals due to **9a** and **9b** isomers overlap in both the ^{31}P{^{1}H} and ^{1}H NMR spectra. **8** = aldehyde **I**, **9** = aldehyde **II**.

mers of the MeCN adducts in the hydride region of the ^1H NMR spectrum at various temperatures indicates equilibrium thermodynamics from a van't Hoff plot ($\ln K_{eq}$ versus $1/T$), and ΔG^0 derived from this represents a weighed average of the free-energy terms for the all isomers. With this caveat, the data indicate that the DPEphos ligand is just as easy to replace in either complex ($\Delta H^0 = \approx(-30 \pm 0.5)$ kJ mol^{-1}) and the process shows an overall large negative change in entropy ($\Delta S^0 = \approx(-90 \pm 3)$ J K^{-1} mol^{-1}), consistent with the addition of a molecule of solvent MeCN in the product. $\Delta G^0(298$ K) values are thus relatively small (<5 kJ mol^{-1}) in favour of the adducts. The adducts **8**[CbCl$_6$] and **9**[CbCl$_6$] do not undergo decarbonylation, as anticipated for complexes in which a vacant site is blocked by a MeCN ligand.

Single crystals of **8a**[CbCl$_6$] were obtained from adding pentane to an acetone solution of the mixture of isomers, and the result of the X-ray structure determination is shown in Figure 6. Dissolution of these crystals gave the equilibri-
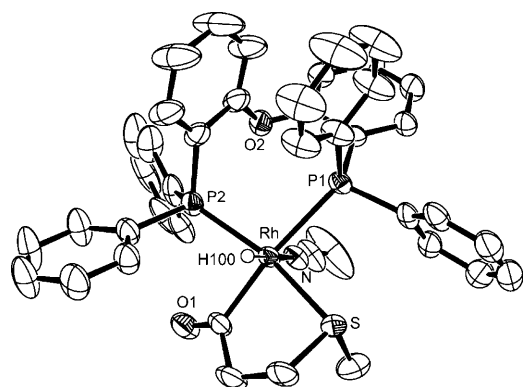

Figure 6. Molecular structure of the cationic portion of **8a**[CbCl$_6$]. Ellipsoids are drawn at the 50% probability level. The anion and hydrogen atoms other than Rh–H are omitted for clarity. Selected bond lengths [Å]: Rh–P1 2.5080(9), Rh–P2 2.305(1), Rh–H(100) 1.49(4), Rh–N 2.129(3), Rh–O1 2.039(4), Rh–S 2.372(1), Rh–O2 3.592(2); selected bond angles [°]: P1-Rh-P2 100.37(3), C-Rh-S, 82.7(1), H(100)-Rh-N 179.0(2).

um mixture observed before. The solid-state structure shows an octahedral Rh^{III} centre with the DPEphos ligand now folded (P1-Rh-P2 100.37(3)°) so that the phosphines lie *cis* to one another and the (located) hydride lies *trans* to the acetonitrile ligand. There is no close Rh···O contact

(3.592(2) Å). The *trans* influence of the acyl group is demonstrated by the differing Rh–P bond lengths: Rh–P1 2.5080(9), Rh–P2 2.305(1) Å.

Complexes **8**[CbCl$_6$] and **9**[CbCl$_6$] represent models for alkene coordination in the catalytic cycle with MeCN replacing the alkene, and in particular the isomers **B** and **C** (Scheme 8), which have a *cis*-disposition of the incoming ligand with respect to the hydride group, are perfectly setup for subsequent insertion into alkene (e.g. structure **C** in Scheme 1). *cis→trans→cis*-folding of the DPEphos ligand as seen here (**5→6→8**) has been noted before in the alcholysis of acyl–palladium complexes bearing this ligand.[25]

Addition of alkene—closing the catalytic cycle: In the preceding sections, it has been demonstrated that addition of aldehyde to the well-defined precatalysts (e.g. **4**[CbCl$_6$]) results in oxidative addition to form acyl hydrides (e.g. **6-**[CbCl$_6$]) in which the hemilabile phosphine ligand stabilises the metal centre towards reductive decarbonylation. MeCN, acting as a model for an incoming alkene, displaces the Rh–O bond and forces the phosphines to lie *cis*. Addition of alkene to complexes **6**[CbCl$_6$] should now close the catalytic cycle.

Addition of methylacrylate to acetone solutions of **6a-**[CbCl$_6$] resulted in the rapid production of an intermediate complex that was short lived ($t_{1/2} = \approx 10$ min) and evolved to give the product complex **11a**[CbCl$_6$] (Scheme 9), which was characterised by NMR spectroscopy and ESIMS/MS. For **6b**[CbCl$_6$], the intermediate was longer lived ($t_{1/2} \approx 30$ min) and has been spectroscopically characterised as **10b**[CbCl$_6$], which then evolved to give **11b**[CbCl$_6$]. The transformation retains mass-balance (Figure 7) and no other complexes of significant concentration are observed by $^{31}P\{^1H\}$ NMR spectroscopy or ESIMS. The final products are discussed first, which were characterised as [Rh(DPEphos)(η^1-MeSC$_2$H$_4$-η^1-COC$_2$H$_4$CO$_2$Me)][CbCl$_6$] (**11a**[CbCl$_6$]) and [Rh(DPEphos)(η^1-MeSC$_6$H$_4$-η^1-COC$_2$H$_4$CO$_2$Me)][CbCl$_6$] (**11b**[CbCl$_6$]).

The room temperature $^{31}P\{^1H\}$ NMR spectrum of **11a-**[CbCl$_6$] shows two broadened environments at $\delta = 42.9$ and 29.7 ppm. These sharpen on cooling to 250 K to give two doublets of doublets at effectively the same chemical shift as at room temperature that show ^{103}Rh–^{31}P and *cis*-^{31}P–^{31}P coupling ($J(PP) = 28$ Hz) consistent with a Rh^I centre ligated with relatively weak donor ligands *trans* to the phosphines ($J(RhP) = 220$ and 173 Hz, respectively). We assign the
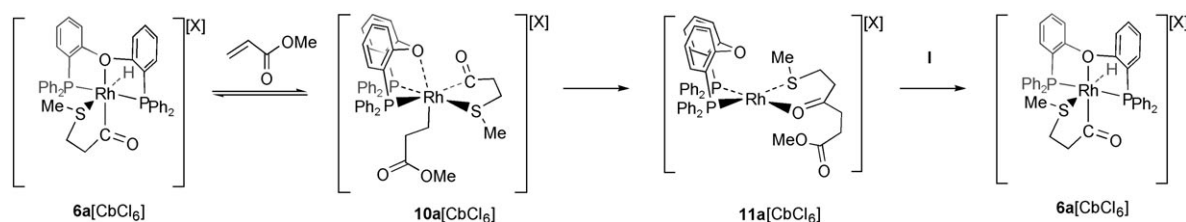
Scheme 9. Addition of methylacylate to **6a**[CbCl$_6$] to give intermediate **10a**[CbCl$_6$] and then final product **16a**[CbCl$_6$]. Addition of aldehyde **I** to **11a**[CbCl$_6$] regenerates **6a**[CbCl$_6$]. The same scheme holds for complex **6b**[CbCl$_6$]. Only one of the possible isomers of **10a**[CbCl$_6$] is shown (see text).
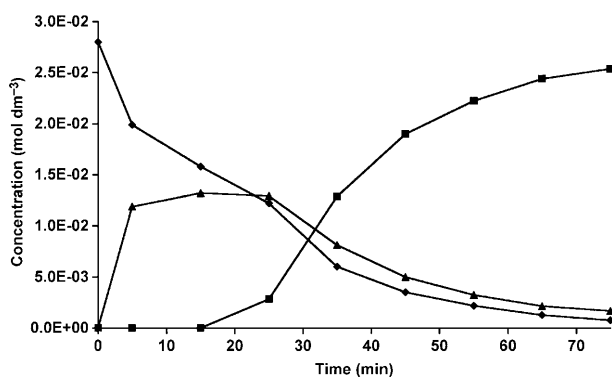
Figure 7. Time/concentration plot for the addition of methylacrylate to **6b**[CbCl$_6$]. ◆ = **6b**[CbCl$_6$]; ▲ = **10b**[CbCl$_6$]; ■ = **11b**[CbCl$_6$].

signal with the larger coupling to a phosphorus *trans* to the bound ketone, which would be expected to be less-strongly bound to the Rh and thus result in a larger J(RhP) coupling constant. Similar RhP couplings are observed for complexes in which η^1-ketones are located *trans* to phosphines or phosphines *trans* to thioethers,[42] and the chemical shifts and J(RhP) coupling constants observed are also very close to those for acetone adduct **4**[CbCl$_6$]. This also suggests that the DPEphos ligand is not bound through the oxygen atom. We discount binding through two η^1-carbonyls on the basis of the difference in J(RhP) coupling and that SMe would find a better match with soft Rh^I than the ester carbonyl. The ^{1}H NMR spectrum shows a featureless hydride region, which demonstrates loss of a hydride ligand, in addition to signals due to the product MeSC$_2$H$_4$COC$_2$H$_4$CO$_2$Me in the aliphatic region. ESIMS displays a parent ion at $m/z =$ 831.13 that loses MeSC$_2$H$_4$COC$_2$H$_4$CO$_2$Me under MS/MS conditions ($m/z = 190.1$) consistent with the suggested formulation. The same NMR and ESIMS spectra are recreated by adding MeSC$_2$H$_4$COC$_2$H$_4$CO$_2$Me to **4**[CbCl$_6$] in acetone. In this case, the molecule is static at room temperature, showing sharp signals in the ^{31}P{^{1}H} NMR spectrum. The broadness observed in the sample in which alkene is added to **6a**[CbCl$_6$] presumably arises from exchange with excess

alkene in solution. Similar spectra are obtained for **11b**-[CbCl$_6$]. Figure 8 shows the MS/MS spectrum showing loss of MeSC$_6$H$_4$COC$_2$H$_4$CO$_2$Me ($m/z = 238.1$) from **11b**[CbCl$_6$] ($m/z = 879.1$). Addition of aldehydes **I** or **II** to acetone solutions of **11a/b**[CbCl$_6$] resulted in the clean formation of complexes **6a**[CbCl$_6$] and **6b**[CbCl$_6$], respectively, which demonstrates turnover of the catalyst.

After having established the identity of **11a/b**[CbCl$_6$], the identity of the intermediate species **10a/b**[CbCl$_6$] was then investigated. For **10a**[CbCl$_6$], this intermediate is only relatively short lived, but for **10b**[CbCl$_6$] it survives long enough for successful characterisation by NMR spectroscopy and ESIMS/MS, presumably a consequence of the constraints imposed by the aryl ring in **II**. These data suggest a sensible formulation for the intermediate species as [Rh-(DPEphos)(CH$_2$CH$_2$CO$_2$Me)(COC$_2$H$_4$SMe)][CbCl$_6$] (**10a**-[CbCl$_6$]) and [Rh(DPEphos)(CH$_2$CH$_2$CO$_2$Me)(COC$_6$H$_4$-SMe)][CbCl$_6$] (**10b**[CbCl$_6$]) (Figure 8). A time/concentration plot shows that the maximum concentration of **10b**[CbCl$_6$] is reached after approximately 15 minutes of reaction time (Figure 7). ESIMS at this time shows a strong-intensity ion at $m/z = 879.2$ that corresponds to the formula suggested for **10b**[CbCl$_6$], as well as peaks due to **6b**[CbCl$_6$] ($m/z = 793.1$). Interrogation of the $m/z = 879.2$ peak by MS/MS resulted in the loss of methylacrylate ($m/z = 86.1$) to give **6b**[CbCl$_6$] ($m/z = 793.1$), presumably by facile β-elimination in the spectrometer under MS/MS conditions (Figure 8). This clearly differentiates this intermediate from the final product **11b**[CbCl$_6$] that has the same mass but fragments by loss of MeSC$_2$H$_6$COC$_2$H$_4$CO$_2$Me on MS/MS ($m/z = 238.1$).

Following the reaction by ^{31}P{^{1}H} and ^{1}H NMR spectroscopy reveals additional data allowing for the tentative identification of the intermediates, which are discussed for **10b**-[CbCl$_6$]. This complex is fluxional at room temperature, displaying broad signals in the ^{1}H and ^{31}P{^{1}H} NMR spectra, in addition to sharper signals due to **6b**[CbCl$_6$] and **11b**-[CbCl$_6$]. The observation of separate signals for **10b**[CbCl$_6$] and **6b**[CbCl$_6$] shows that they are not in rapid equilibrium on the NMR timescale with each other. Cooling a sample to 200 K gave a complicated ^{1}H NMR spectrum in the aliphatic
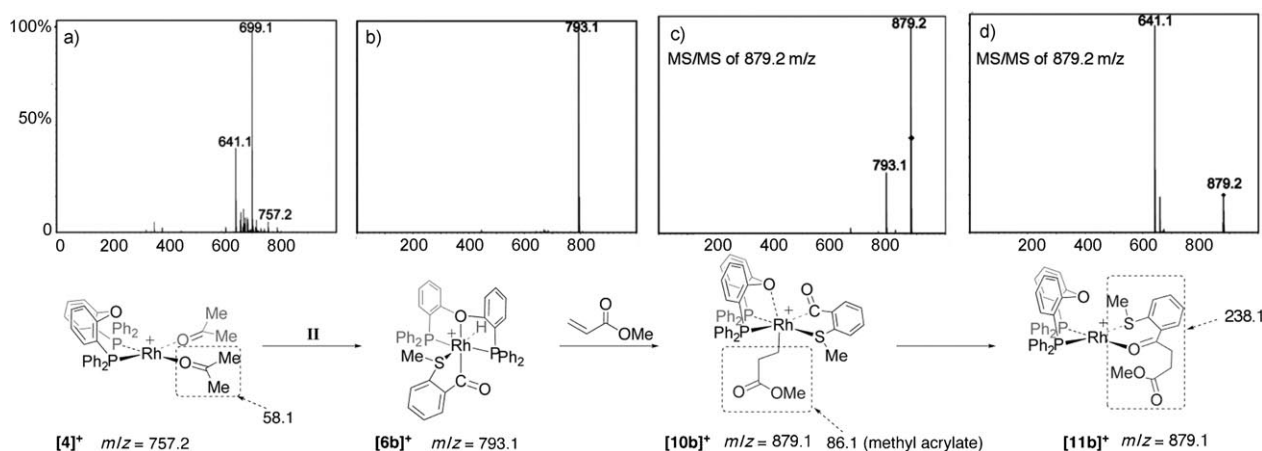

Figure 8. ESI (a,b) and ESIMS/MS (c,d) data for the sequential addition of aldehyde **II** to **4**[CbCl$_6$].

region, with overlapping signals. In the hydride region, only a diminished signal due to **6b**[CbCl$_6$] was observed, which demonstrated that the intermediate species does not have a hydride ligand, and suggested that hydride insertion into the alkene has taken place. In the ^{31}P{^{1}H} NMR spectrum, six doublets of doublets were observed, in addition to the signal for **6b**[CbCl$_6$], which we assign to three isomers of **10b**-[CbCl$_6$] in which the alkyl, acyl and thioether ligands sit in different, mutually *cis*, positions around an octahedral Rh^{III} centre. These isomers are observed in the ratio 5:3:2, facilitating the pairing of resonances. All the pairs show *cis* *J*(PP) coupling (26–32 Hz]). For two of these pairs, there is one large and one small *J*(RhP) coupling (for example, 174 and 79 Hz) and the third shows two small values ($\approx$75 Hz). This is reminiscent of the couplings observed in the MeCN adducts (e.g. **8b**[CbCl$_6$]) and suggests phosphines that are either opposite a high *trans* influence ligand (alkyl or acyl: small *J*(RhP)) or the thioether group (larger *J*(RhP)). The DPEphos oxygen atom is suggested to provide stabilisation to the, formally, 16-electron Rh^{III} centre, but as these isomers interconvert at room temperature, any Rh−O interaction is likely to be weak, allowing access to a five-coordinate, fluxional intermediate. Reductive elimination from **10b**[CbCl$_6$] to form **11b**[CbCl$_6$] would also require a five-coordinate species.[8,9] Alkyl-acyl species have been reported previously, but as found here, they often undergo reductive elimination to give the corresponding ketones.[44]

The complete hydroacylation catalytic cycle from observable intermediates: Although a rigorous kinetic study is outside the scope of this paper, the reactivity and new complexes reported that arise from stoichiometric addition of substrates to precatalyst species allows a catalytic cycle to be presented based upon observed species. Scheme 10 presents the cycle and shows the flexible role of the hemilabile ligand in accommodating the various metal electron counts, oxidation states and resulting geometries. This cycle complements similar schemes outlined by Bosnich,[2a] which have been computationally studied by Morehead and Sargent[3] for the intramolecular hydroacylation of 4-pentenals, and intermolecular hydroacylation reactions by using [M(η^5-C$_5$Me$_4$X)(η^2-H$_2$C=CHSiMe$_3$)$_2$] catalysts (X=Me, CH$_3$; M=Co,[4] Rh[5]) as reported by Brookhart.

Applications to organic synthesis—representative examples: Employing the DPEphos catalyst in the benchmark hydroacylation reaction indicated a modest advantage over the Bosnich dppe-derived catalyst (see the section Evaluation of precatalysts in a benchmark hydroacylation reaction). However, this benchmark reaction is achievable with a number of catalysts and the test of whether the DPEphos-derived system had any real advantages in terms of reactivity would be to employ it in more challenging hydroacylation reactions. Accordingly, the DPEphos catalyst was used in a series of hydroacylation reactions between β-S-substituted aldehydes **I**, **II**, **V** and **VI** (Table 3), the two alkenes methyl acrylate and octene, and a terminal and internal alkyne. The
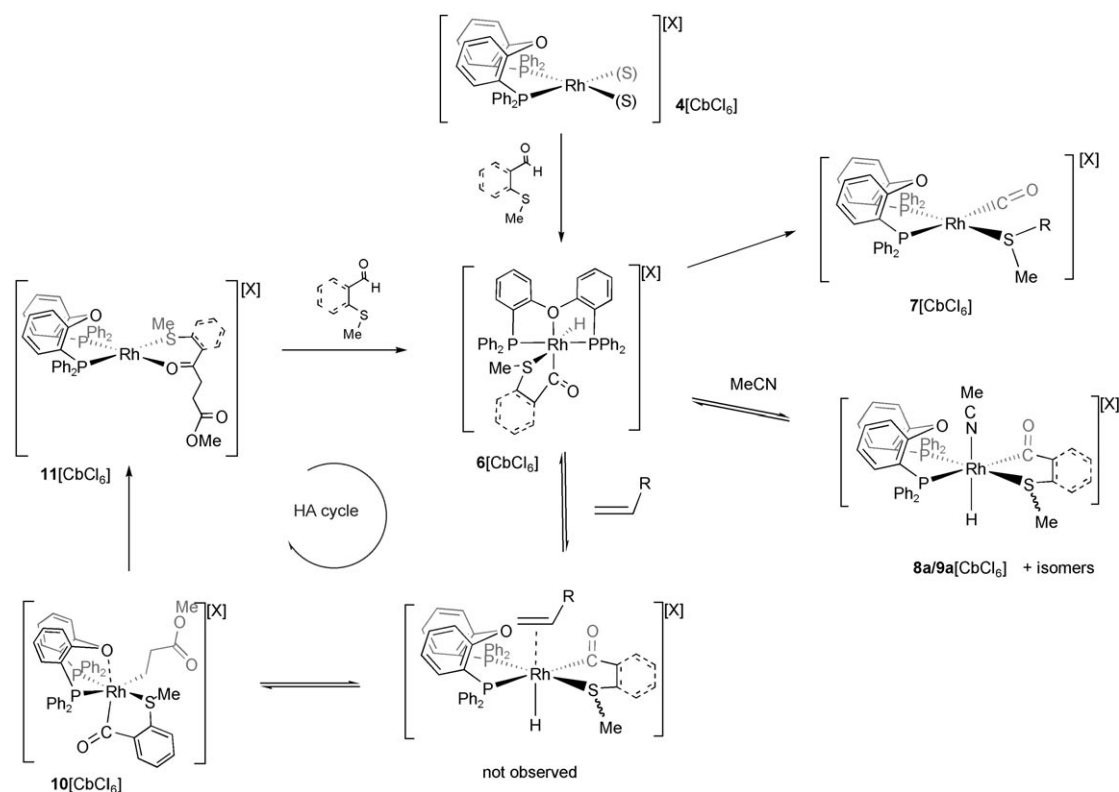
Scheme 10. Catalytic cycle, decarbonylation products and acetontrile adducts for the hydroacylation reaction by using **4**[CbCl$_6$], aldehyde **I** or **II** and methylacrylate.

catalyst used in these reactions was generated from the simple combination of [RhCl(cod)]₂, DPEphos and Ag-[ClO₄]. The perchlorate counterion was selected as a partner to the cationic fragment from a pragmatic view, considering the lack of general availability of the alternative carborane derived systems. The results are presented in Table 3; all combinations of coupling partners delivered good yields of the hydroacylation adducts. In all cases, the yields achieved matched, or surpassed, those obtained with the dppe-containing catalyst.[20] Particularly worthy of note are the reactions of all four aldehydes with the simple alkene octene (entries 4, 8, 12 and 16); use of the dppe-derived catalyst in these reactions delivered very poor yields (<5%) of hydroacylation adducts, at best. For example, the reactions of both aldehydes **V** and **VI** with octene deliver none of the hydroacylation adducts with this catalyst. No doubt key in this marked performance gain with these challenging substrates compared with the dppe ligated system is the longevity of the catalyst with regard to reductive decarbonylation. Although we suggest the overall rate of reaction might not be significantly faster with the DPEphos systems (c.f. the broadly similar reaction times observed in the benchmark reaction) it is the catalyst robustness that allows continued turnover over a long period of time (up to 48 h). Consistent with this, at the end of catalysis under the benchmark conditions, addition of **II** to the reaction mixture regenerates **6b**[CbCl₆] as the only observable organometallic product, which demonstrates that post catalysis the catalyst is available for further turnovers and has not decomposed significantly.

Counterion effects: Although the stoichiometric additions of aldehydes and alkenes to the precursor complexes show no significant difference on changing the counterion, a comparison of the performance of various precursor complexes reveals that there is an appreciable counterion effect (Table 4) in the benchmark catalysis. Counterion effects in catalysis are well documented and can result from a combination of enhanced metal vacant site availability and attenuation of

Table 3. Scope of the new catalyst system.[a]

Entry	Aldehyde	Alkene/alkyne	Product	t [h]	Yield [%][b]
1				1	74
2	MeS, O, H (**I**)			2	82
3		Me≡Ph		16	80
4				24	67
5				16	81
6	EtS, Me, O, H (**V**)			16	97
7		Me≡Ph		24	73
8				48	61
9				4	75
10	S, S, O, H (**VI**)			4	83
11		Me≡Ph		24	81
12				48	89
13				2	86
14	MeS, O, H (**II**)			2	91
15		Me≡Ph		24	81
16				24	73

[a] Conditions: aldehyde (1.0 equiv), alkene or alkyne (2.0 equiv), [RhCl(cod)]₂ (2.5 mol%), DPEphos (5 mol%), Ag[ClO₄] (5 mol%), acetone, 55 °C. [b] Isolated yields of single isomers.

Table 4. Counterion influence on benchmark reaction (see Table 1).[a]

Entry	Catalyst	Conversion [%][b]	t
1	[Rh(dppe)(nbd)][ClO$_4$]	100	90 min
2	[Rh(DPEphos)(nbd)][ClO$_4$]	100	60 min
3	[Rh(DPEphos)(nbd)][PF$_6$]	100	4 h
4	[Rh(DPEphos)(nbd)][BAr$^F_4$]	100	75 min
5	[Rh(DPEphos)(nbd)] [closo-CB$_{11}$H$_6$Cl$_6$]	100	30 min
6	[Rh(DPEphos)(nbd)] [closo-CB$_{11}$H$_6$Br$_6$]	100	45 min

[a] Conditions: aldehyde (1.0 equiv), methyl acrylate (2.0 equiv), catalyst (5 mol.%), acetone, 55°C. Catalyst generated by addition of H$_2$ (1 atm, 5 min, acetone). [b] Determined by ^{1}H NMR spectroscopy.

decomposition pathways by the anion.[45] Under bench-top conditions, the carborane anions perform the best (entries 5 and 6), as measured by time taken for the reaction to reach completion, with [BAr$^F_4$]$^-$ performing less well (entry 4), and [PF$_6$]$^-$ significantly poorer (entry 3). This could well be due to trace amounts of water present in the acetone that have been shown to attenuate the activity of [BAr$^F_4$]$^-$ and, more so, [PF$_6$]$^-$ salts in hydrogenation reactions with cationic Group 9 metals.[28,46] Overall, salts of [ClO$_4$]$^-$ represent a reasonable balance of convenience and overall rate (entry 2).

Conclusions

We have developed a practicable catalyst for the hydroacylation reaction of β-S-substituted aldehydes with activated and unactivated alkenes and alkynes. The catalyst system uses a hemilabile DPEphos ligand to stabilise key acyl–hydrido intermediates against unproductive reductive decarbonylation. This leads to a longer-lived catalyst that is able to couple relatively unreactive alkenes, such as 1-octene, with the aldehyde. Stoichiometeric studies on sequential addition of aldehyde and alkene to precatalyst systems shows that DPEphos provides not only stabilisation towards reductive decarbonylation through reversible coordination of the oxygen ligand, but can also adjust its coordination geometry (*cis, trans, cis*). This not only reflects the requirements of the rhodium centre throughout the catalytic cycle but also allows coordinated groups (hydride, acyl and alkene) to adopt mutually *cis* orientations necessary for the key insertion and reductive elimination steps. The flexible and hemilabile nature of the ligand is thus important, and these design features could well be significant in the realisation of future catalyst systems that will be able to couple any aldehyde with any alkene—the ultimate goal in the area of hydroacylation chemistry.

Acknowledgement

[1] a) J. W. Suggs, *J. Am. Chem. Soc.* **1978**, *100*, 640–641; b) K. Sakai, J. Ide, 0. Oda, N. Nakamura, *Tetrahedron Lett.* **1972**, 1287-1290.

[2] a) D. P. Fairlie, B. Bosnich, *Organometallics* **1988**, *7*, 946–954; b) This catalyst has been formulated as existing mainly as monomeric [Rh(acetone)$_2$(dppe)][ClO$_4$] in dilute acetone solutions, the closely associated ion-pair [Rh(ClO$_4$)(dppe)] in CD$_2$Cl$_2$ solutions and the arene bridged dimer [Rh(dppe)]$_2$[ClO$_4$]$_2$ in nitromethane. The active catalyst is strongly argued to be a monomeric substrate adduct, and rates of catalysis for the hydroacylation of 4-pentenal are similar for all three solvents, which suggests a common active species.

[3] I. F. D. Hyatt, H. K. Anderson, A. T. Morehead, A. L. Sargent, *Organometallics* **2008**, *27*, 135–147.

[4] C. P. Lenges, P. S. White, M. Brookhart, *J. Am. Chem. Soc.* **1998**, *120*, 6965–6979.

[5] A. H. Roy, C. P. Lenges, M. Brookhart, *J. Am. Chem. Soc.* **2007**, *129*, 2082–2093.

[6] R. H. Crabtree, *The Organometallic Chemistry of the Transition Metals*, Wiley, Hoboken, New Jersey, **2005**.

[7] R. Goikhman, D. Milstein, *Angew. Chem.* **2001**, *113*, 1153–1156; *Angew. Chem. Int. Ed.* **2001**, *40*, 1119–1122.

[8] a) U. Fekl, K. I. Goldberg, *J. Am. Chem. Soc.* **2002**, *124*, 6804–6805; b) J. Procelewska, A. Zahl, G. Liehr, R. van Eldik, N. A. Smythe, B. S. Williams, K. I. Goldberg, *Inorg. Chem.* **2005**, *44*, 7732–7742; c) A. T. Luedtke, K. I. Goldberg, *Inorg. Chem.* **2007**, *46*, 8496–8498.

[9] D. Milstein, *Acc. Chem. Res.* **1984**, *17*, 221–226.

[10] B. Bosnich, *Acc. Chem. Res.* **1998**, *31*, 667–674.

[11] C. H. Jun, E. A. Jo, J. W. Park, *Eur. J. Org. Chem.* **2007**, 1869–1881.

[12] D. Milstein, *J. Chem. Soc. Chem. Commun.* **1982**, 1357–1358.

[13] D. P. Fairlie, B. Bosnich, *Organometallics* **1988**, *7*, 936–945.

[14] B. R. James, C. G. Young, *J. Chem. Soc. Chem. Commun.* **1983**, 1215–1216.

[15] a) R. W. Barnhart, D. A. McMorran, B. Bosnich, *Chem. Commun.* **1997**, 589–590; b) R. W. Barnhart, D. A. McMorran, B. Bosnich, *Inorg. Chim. Acta* **1997**, *263*, 1–7; c) R. W. Barnhart, B. Bosnich, *Organometallics* **1995**, *14*, 4343–4348; d) R. W. Barnhart, X. Wang, P. Noheda, S. H. Bergens, J. Whelan, B. Bosnich, *J. Am. Chem. Soc.* **1994**, *116*, 1821–1830.

[16] a) K. Tanaka, G. C. Fu, *J. Am. Chem. Soc.* **2001**, *123*, 11492–11493; b) K. Tanaka, G. C. Fu, *Angew. Chem.* **2002**, *114*, 1677–1679; *Angew. Chem. Int. Ed.* **2002**, *41*, 1607–1609; c) H. D. Bendorf, C. M. Colella, E. C. Dixon, M. Marchetti, A. N. Matukonis, J. D. Musselman, T. A. Tiley *Tetrahedron Letters* **2002**, *43*, 7031–7034.

[17] a) C.-H. Jun, Y.-G. Lim, *Tetrahedron Lett.* **1995**, *36*, 3357–3360; b) C.-H. Jun, H. Lee, J.-B. Hong, *J. Org. Chem.* **1997**, *62*, 1200–1201; c) C.-H. Jun, J.-B. Hong, D.-Y. Lee, *Synlett* **1999**, 1–12; C.-H. Jun, J.-B. Hong, Y.-H. Kim, K.-Y. Chung, *Angew. Chem.* **2000**, *112*, 3582–3584; *Angew. Chem. Int. Ed.* **2000**, *39*, 3440–3442; d) C.-H. Jun, D.-Y. Lee, H. Lee, J.-B. Hong, *Angew. Chem.* **2000**, *112*, 3214–3216; *Angew. Chem. Int. Ed.* **2000**, *39*, 3070–3072; e) C.-H. Jun, H. Lee, S.-G. Lim, *J. Am. Chem. Soc.* **2001**, *123*, 751–752; f) C. H. Jun, J. H. Chung, D. Y. Lee, A. Loupy, S. Chatti, *Tetrahedron Lett.* **2001**, *42*, 4803–4805; g) C. H. Jun, H. Lee, S. G. Lim, *J. Am. Chem. Soc.* **2001**, *123*, 751–752; h) C.-H. Jun, H. Lee, J.-B. Hong, B.-I. Kwon, *Angew. Chem.* **2002**, *114*, 2250–2251; *Angew. Chem. Int. Ed.* **2002**, *41*, 2146–2147; i) C.-H. Jun, C. W. Moon, D.-Y. Lee, *Chem. Eur. J.* **2002**, *8*, 2422–2428; j) C.-H. Jun, C. W. Moon, H. Lee, D.-Y. Lee, *J. Mol. Catal. A: Chem.* **2002**, *189*, 145–156; k) C.-H. Jun, C. W. Moon, S.-G. Lim, H. Lee, *Org. Lett.* **2002**, *4*, 1595–1597; l) C.-H. Jun, J. H. Lee, *Pure Appl. Chem.* **2004**, *76*, 577–587; m) Y. Taura, M. Tanaka, X. M. Wu, K. Funakoshi, K. Sakai, *Tetrahedron* **1991**, *47*, 4879–4888; n) M. Tanaka, M. Imai, M. Fujio, E. Sakamoto, M. Takahashi, Y. Eto-Kato, X. M. Wu, K. Funakoshi, K. Sakai, H. Suemune, *J. Org. Chem.* **2000**, *65*, 5806–5816; o) M. Tanaka, M. Takahashi, E. Sakamoto, M. Imai, A. Matsui, M. Fujio, K. Funakoshi, K. Sakai, H. Suemune, *Tetrahedron* **2001**, *57*, 1197–1204; p) M. Tanaka, M. Imai, Y. Yamamoto, K. Tanaka, M. Shimowatari, S. Nagumo, N. Kawahara, H. Suemune, *Org. Lett.* **2003**, *5*, 1365–1367; q) M. Tanaka, K. Sakai, H. Suemune, *Current Organic Chemistry* **2003**, *7*, 353–367;

r) K. Tanaka, M. Tanaka, H. Suemune, *Tetrahedron Lett.* **2005**, *46*, 6053–6056; s) K. Tanaka, Y. Shibata, T. Suda, Y. Hagiwara, M. Hirano, *Org. Lett.* **2007**, *9*, 1215–1218; t) M. Imai, M. Tanaka, S. Nagumo, N. Kawahara, H. Suemune, *J. Org. Chem.* **2007**, *72*, 2543–2546; u) Y. Oonishi, M. Mori, Y. Sato, *Synthesis* **2007**, 2323–2336.

[18] a) M. C. Willis, S. Sapmaz, *Chem. Commun.* **2001**, 2558–2559; b) M. C. Willis, S. J. McNally, P. J. Beswick, *Angew. Chem.* **2004**, *116*, 344–347; *Angew. Chem. Int. Ed.* **2004**, *43*, 340–343; c) M. C. Willis, H. E. Randell-Sly, R. L. Woodward, G. S. Currie, *Org. Lett.* **2005**, *7*, 2249–2251.

[19] G. L. Moxham, H. E. Randell-Sly, S. K. Brayshaw, R. L. Woodward, A. S. Weller, M. C. Willis, *Angew. Chem.* **2006**, *118*, 7780–7784; *Angew. Chem. Int. Ed.* **2006**, *45*, 7618–7622.

[20] M. C. Willis, H. E. Randell-Sly, R. L. Woodward, S. J. McNally, G. S. Currie, *J. Org. Chem.* **2006**, *71*, 5291–5297.

[21] a) C. F. Lochow, R. G. Miller, *J. Am. Chem. Soc.* **1976**, *98*, 1281–1283; b) R. E. Campbell, C. F. Lochow, K. P. Vora, R. G. Miller, *J. Am. Chem. Soc.* **1980**, *102*, 5824–5830; c) T. B. Marder, D. C. Roe, D. Milstein, *Organometallics* **1988**, *7*, 1451–1453.

[22] P. Braunstein, F. Naud, *Angew. Chem.* **2001**, *113*, 702–722; *Angew. Chem. Int. Ed.* **2001**, *40*, 680–699.

[23] a) J. C. Jeffery, T. B. Rauchfuss, P. A. Tucker, *Inorg. Chem.* **1980**, *19*, 3306–3316; b) J. W. Faller, N. Sarantopoulos, *Organometallics* **2004**, *23*, 2008–2014; c) G. Chen, W. H. Lam, W. S. Fok, H. W. Lee, F. Y. Kwong, *Chem. Asian J.* **2007**, *2*, 306–313; d) D. B. Grotjahn, Y. Gong, L. Zakharov, J. A. Golen, A. L. Rheingold, *J. Am. Chem. Soc.* **2006**, *128*, 438–453; e) S. Chikkali, D. Gudat, M. Niemeyer, *Chem. Commun.* **2007**, 981–983; f) H. Werner, *Dalton Trans.* **2003**, 3829–3837; g) N. C. Gianneschi, M. S. Masar, C. A. Mirkin, *Acc. Chem. Res.* **2005**, *38*, 825–837; h) P. A. Ulmann, A. M. Brown, M. V. Ovchinnikov, C. A. Mirkin, A. G. DiPasquale, A. L. Rheingold, *Chem. Eur. J.* **2007**, *13*, 4529–4534; i) T. E. Barder, S. D. Walker, J. R. Martinelli, S. L. Buchwald, *J. Am. Chem. Soc.* **2005**, *127*, 4685–4696; j) Z. Q. Weng, S. H. Teo, T. S. A. Hor, *Acc. Chem. Res.* **2007**, *40*, 676–684; k) M. H. Chisholm, J. C. Gallucci, G. Yaman, *Chem. Commun.* **2006**, 1872–1874.

[24] A. J. Sandee, L. A. van der Veen, J. N. H. Reek, P. C. J. Kamer, M. Lutz, A. L. Spek, P. van Leeuwen, *Angew. Chem.* **1999**, *111*, 3428–3432; *Angew. Chem. Int. Ed.* **1999**, *38*, 3231–3235.

[25] P. W. N. M. van Leeuwen, M. A. Zuideveld, B. H. G. Swennenhuis, Z. Freixa, P. C. J. Kamer, K. Goubitz, J. Fraanje, M. Lutz, A. L. Spek, *J. Am. Chem. Soc.* **2003**, *125*, 5523–5539.

[26] R. Venkateswaran, J. T. Mague, M. S. Balakrishna, *Inorg. Chem.* **2007**, *46*, 809–817.

[27] a) C. A. Reed, *Acc. Chem. Res.* **1998**, *31*, 133–139; b) N. J. Patmore, C. Hague, J. H. Cotgreave, M. F. Mahon, C. G. Frost, A. S. Weller, *Chem. Eur. J.* **2002**, *8*, 2088–2098; c) A. Rifat, N. J. Patmore, M. F. Mahon, A. S. Weller, *Organometallics* **2002**, *21*, 2856–2865.

[28] G. L. Moxham, T. M. Douglas, S. K. Brayshaw, G. Kociok-Kohn, J. P. Lowe, A. S. Weller, *Dalton Trans.* **2006**, 5492–5505.

[29] M. Utsunomiya, R. Kuwano, M. Kawatsura, J. F. Hartwig, *J. Am. Chem. Soc.* **2003**, *125*, 5608–5609.

[30] W. Lesueur, E. Solari, C. Floriani, A. ChiesiVilla, C. Rizzoli, *Inorg. Chem.* **1997**, *36*, 3354–3362.

[31] a) J. C. Lewis, J. Wu, R. G. Bergman, J. A. Ellman, *Organometallics* **2005**, *24*, 5737–5746; b) Y. Zhang, J. C. Lewis, R. G. Bergman, J. A. Ellman, E. Oldfield, *Organometallics* **2006**, *25*, 3515–3519.

[32] P. S. Pregosin, R. W. Kunz, *NMR of transition metal phosphine complexes* **1979**, Springer-Verlag, Berlin

[33] a) J. A. Long, T. B. Marder, P. E. Behnken, M. F. Hawthorne, *J. Am. Chem. Soc.* **1984**, *106*, 2979–2989; b) I. V. Kourkine, C. S. Slone, C. A. Mirkin, L. M. Liable-Sands, A. L. Rheingold, *Inorg. Chem.* **1999**, *38*, 2758–2759.

[34] R. R. Schrock, J. A. Osborn, *J. Am. Chem. Soc.* **1976**, *98*, 2134–2143.

[35] N. W. Alcock, J. M. Brown, J. C. Jeffery, *J. Chem. Soc. Dalton Trans.* **1976**, 583–588.

[36] K. Wang, T. J. Emge, A. S. Goldman, C. Li, S. P. Nolan, *Organometallics* **1995**, *14*, 4929–4936.

[37] a) D. Milstein, W. C. Fultz, J. C. Calabrese, *J. Am. Chem. Soc.* **1986**, *108*, 1336–1338; b) C. Bianchini, A. Meli, M. Peruzzini, F. Vizza, F. Bachechi, *Organometallics* **1991**, *10*, 820–823; c) M. A. Garralda, R. Hernandez, L. Ibarlucea, E. Pinilla, M. R. Torres, M. Zarandona, *Organometallics* **2007**, *26*, 1031–1038.

[38] Y. S. Varshavsky, T. G. Cherkasova, N. A. Buzina, L. S. Bresler, *J. Organomet. Chem.* **1994**, *464*, 239–245.

[39] B. K. Corkey, F. L. Taw, R. G. Bergman, M. Brookhart, *Polyhedron* **2004**, *23*, 2943–2954.

[40] a) E. W. Abel, S. K. Bhargava, K. G. Orrell, *Prog. Inorg. Chem.* **1984**, *32*, 1–118; b) E. W. Abel, G. W. Farrow, K. G. Orrell, *J. Chem. Soc. Dalton Trans.* **1976**, 1160–1163; c) E. W. Abel, M. Booth, K. G. Orrell, *J. Chem. Soc. Dalton Trans.* **1980**, 1582–1592; d) F. Qian, M. Ferrer, M. L. H. Green, P. Mountford, V. S. B. Mtetwa, K. Prout, *J. Chem. Soc. Dalton Trans.* **1991**, 1397–1406; e) J. R. Dilworth, C. A. M. von Beckh, S. I. Pascu, *Dalton Trans.* **2005**, 2151–2161.

[41] X. P. Shan, J. H. Espenson, *Organometallics* **2003**, *22*, 1250–1254, and references therein.

[42] a) S. Sjovall, C. Andersson, O. F. Wendt, *Organometallics* **2001**, *20*, 4919–4926; b) A. M. Brown, M. V. Ovchinnikov, C. A. Mirkin, *Angew. Chem.* **2005**, *117*, 4279–4281; *Angew. Chem. Int. Ed.* **2005**, *44*, 4207–4209; c) Y. M. Jeon, J. Heo, A. M. Brown, C. A. Mirkin, *Organometallics* **2006**, *25*, 2729–2732.

[43] In our initial communication (reference [19]), we did not report the minor isomer **8c**[CbCl$_6$] present in 5% relative concentration at 289 K.

[44] a) C. P. Casey, D. M. Scheck, *J. Am. Chem. Soc.* **1980**, *102*, 2723–2728; b) J. W. Suggs, M. J. Wovkulich, S. D. Cox, *Organometallics* **1985**, *4*, 1101–1107; c) K. I. Goldberg, R. G. Bergman, *Organometallics* **1987**, *6*, 430–432.

[45] a) Y. X. Chen, T. J. Marks, *Chem. Rev.* **2000**, *100*, 1391–1434; b) A. Macchioni, *Chem. Rev.* **2005**, *105*, 2039–2073; c) P. S. Pregosin, P. G. A. Kumar, I. Fernández, *Chem. Rev.* **2005**, *105*, 2977–2998.

[46] S. P. Smidt, N. Zimmermann, M. Studer, A. Pfaltz, *Chem. Eur. J.* **2004**, *10*, 4685–4693.